ORIGINAL ARTICLE

Response surface optimization of biodiesel synthesis over a novel biochar-based heterogeneous catalyst from cultivated (*Musa sapientum*) banana peels

Jakkrapong Jitjamnong[1] · Chachchaya Thunyaratchatanon[2] · Apanee Luengnaruemitchai[2,3] · Napaphat Kongrit[1] · Naparat Kasetsomboon[1] · Arrisa Sopajarn[4] · Narinphop Chuaykarn[5] · Nonlapan Khantikulanon[6]

Abstract
In this work, response surface methodology (RSM) was utilized to optimize the biodiesel yield of the transesterification reaction. A novel solid carbon-supported potassium hydroxide catalyst derived from the pyrolysis of cultivated banana (*Musa sapientum*) peels and potassium carbonate (K_2CO_3) was used as the catalyst for biodiesel production. A five-level (-2, -1, 0, $+1$, and $+2$) RSM with a four-factor central composite design of independent variable factors (methanol to palm oil molar ratio (6:1–18:1), catalyst loading (3–7 wt.%), reaction time (30–150 min), and reaction temperature (50–70 °C)) were randomly setup using the Design of Experiment program. The 30 wt.% K_2CO_3 catalyst calcined at 600 °C under atmosphere pressure exhibited the highest catalytic activity, since the pyrolysis ash was rich in K that formed a basic heterogeneous catalyst. Within the range of selected operating conditions, the optimized methanol:oil molar ratio, catalyst loading, reaction time, and reaction temperature were found to be 15:1, 4 wt.%, 120 min, and 65 °C, respectively, to give a biodiesel yield of 99.16%. The actual biodiesel yield of 98.91% was obtained under the predicted optimal conditions. The high R^2 (96.76%) and R^2_{adj} (92.97%) values indicated that the fitted model showed a good agreement with the predicted and actual biodiesel yield.

Keywords Cultivated banana peels · Biodiesel · Transesterification · Heterogeneous catalyst · Response surface methodology (RSM)

1 Introduction

The rapidly increasing emissions of greenhouse gases and other pollutants, such as carbon dioxide (CO_2), carbon monoxide, oxides of sulfur (SO_x), and oxides of nitrogen (NO_x), and particulates, in the world have a harmful impact on human life. Biodiesel, typically fatty acid methyl esters (FAMEs), has

several environmental benefits when compared with petroleum-based diesel, including that it is sustainably renewable, biodegradable, has a clean combustion, a higher flash point, is derived from eco-friendly energy resources, and is environmentally acceptable in diesel engines [1, 2]. Commercial biodiesel production is obtained by the transesterification of oil (vegetable oils, animal fats, algae,

✉ Jakkrapong Jitjamnong
alekjakkrapong@gmail.com

1 Department of Petroleum Technology, Faculty of Industrial Education and Technology, Rajamangala University of Technology Srivijaya, 2/1 Rachadamnoennork Rd., Boryang, Muang, Songkhla 90000, Thailand

2 The Petroleum and Petrochemical College, Chulalongkorn University, Pathumwan, Bangkok 10330, Thailand

3 Center of Excellence in Catalysis for Bioenergy and Renewable Chemicals (CBRC), Chulalongkorn University, Bangkok 10330, Thailand

4 Department of Agricultural Machinery Technology, Rattaphum College, Rajamangala University of Technology Srivijaya, Rattaphum, Songkhla 90180, Thailand

5 Department of Food and Nutrition, Faculty of Liberal Arts, Rajamangala University of Technology Srivijaya, 1 Rachadamnoennork Rd., Boryang, Muang, Songkhla 90000, Thailand

6 Department of Environmental Health, Faculty of Public Health, Valaya Alongkorn Rajabhat University, Khlong 1, Khlong Luang, Pathum Thani 10120, Thailand

and waste cooking oils) and an alcohol (usually methanol or ethanol) in the presence of a suitable catalyst for producing the fatty acid alkyl.

Conventionally, biodiesel is synthesized using a homogeneous base catalyst, such as potassium hydroxide (KOH) or sodium hydroxide (NaOH) [3–6]. However, the drawbacks of base-homogeneous catalysts are the difficulty in the separation of catalyst from the organic phase, the undesirable soap formation from free fatty acids, and the production of a large amount (10% of the biodiesel volume) of contaminated wastewater requiring treatment before disposal. An alternative to homogeneous catalysts for biodiesel synthesis is the use of solid-supported heterogeneous catalysts. The benefits of such heterogeneous catalysts are that they are easily separated from the product, reduce the amount of soap produced, have a relatively long catalytically active time, and are non-corrosive [7–10].

Recently, to reduce the biodiesel synthesis cost, appropriate heterogeneous catalysts have been derived from biomass waste materials, such as banana peels [11–15], wood [8, 16], cocoa pod husk [17, 18], coconut husk [19], rice husk [20–22], peanut shell [23], pomelo peel [24], tucumã peel [25], waste cupuaçu [26], walnut shell [27], kola nut pod [28], and banana peduncle [29, 30]. The use of 30 wt.% of calcium oxide (CaO) loaded on the rice husk ash for biodiesel production from palm oil gave a biodiesel (FAME) yield of 91.5% when using the catalyst at 7 wt.%, a methanol:oil molar ratio of 9:1, and a 65 °C reaction for 4 h [20]. With respect to the effect of the CaO loading level on the rice husk biochar as a catalyst in the transesterification reaction, the optimum biodiesel yield was obtained with 30 wt.% of CaO to give a maximum FAME yield of 93.4% when using a 8 wt.% catalyst loading, methanol:palm oil molar ratio of 9:1, and a 65 °C reaction for 180 min [21]. Likewise, for peat biochar-supported CaO catalysts, the 30 wt.% CaO demonstrated the best performance with a biodiesel yield of 93.4% when the reaction was performed with a catalyst loading of 5 wt.%, methanol:oil molar ratio of 8:1 and a 65 °C reaction for 150 h [31].

Currently, the use of biochar loading with different potassium salts, such as potassium carbonate (K_2CO_3), for biodiesel production has gained interest [24, 32–34]. Biochar as a precursor for activated porous carbon has been studied, where it was synthesized by the thermal decomposition of biomass [21]. Biochar ash-based solid catalysts show a good catalytic activity, are environmentally friendly, and renewable for biodiesel production [20]. A novel pyrolyzed pomelo peel-supported alkaline (K_2CO_3) catalyst was used in the transesterification of palm oil to obtain a FAME yield of 98% at the optimum condition of a 65 °C reaction for 2.5 h with an 8:1 methanol:palm oil molar ratio and 6 wt.% of catalyst [24]. With respect to the effect of the K_2CO_3 loading level on a solid peat waste as the support to prepare a carbon solid base catalyst for biodiesel production, a K_2CO_3 loading of 30 wt.% supported on the biochar gave the highest catalytic

Table 1 Physiochemical properties of the palm oil used in this study

Property	Unit	Value
Density at 15 °C	kg/m^3	890
Viscosity at 40 °C	mm^2/s	37.6
Free fatty acid	wt.%	–
Triglyceride (%)	wt.%	97.54
Diglyceride (%)	wt.%	2.46
Monoglycerde (%)	wt.%	–
Ester	wt.%	–

activity with a maximum biodiesel yield of 98.6% at a catalyst loading of 5 wt.%, methanol:oil molar ratio of 8:1, and a 65 °C reaction for 150 min [32].

Banana is the second largest tropical fruit produced in the world, causing an extensive supply of its waste by-product (banana peel). Cultivated banana (*Musa sapientum*) plants are commonly found in many parts of Thailand, and all parts of a banana plant can be utilized. The non-edible banana peel has been used in various applications, such as bio-sorbents, bioethanol production, and other energy-related activities [13, 15]. Recently, the use of banana peel biochar as a catalyst for biodiesel production has become of great interest. The use of banana peel was chosen in this study because it contains various minerals and nutrients, including the metal cations of calcium (Ca), sodium, potassium (K), iron, magnesium, plus anions of sulfur [11, 15, 35].

There are several operating process parameters for biodiesel production through the transesterification reaction, such as the methanol:oil molar ratio, catalyst loading level, reaction temperature, reaction time, and agitation speed [36]. In addition, response surface methodology (RSM) via a central composite design (CCD) as a statistical tool has been applied for developing and optimizing the influencing parameters to achieve the desired output with a reduced number of experimental runs [37]. For example, after using RSM to optimize the operating parameters, a 95.25% biodiesel yield was obtained for *Thevetia peruviana* (yellow oleander) oil, while, likewise, a maximum biodiesel

Table 2 Independent factors used for CCD in transesterification with the 30K/BP-600 catalyst

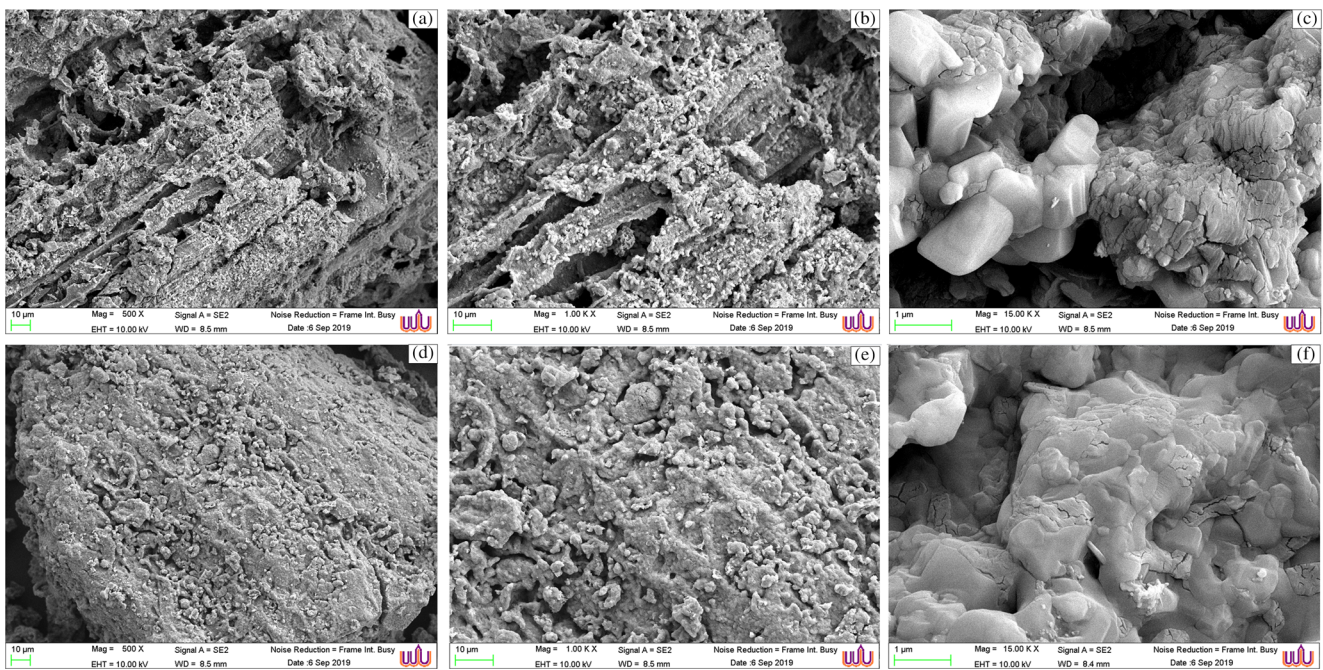| Factor	Unit	Symbol	Coded factor level				
			−2	−1	0	+1	+2
Methanol:oil molar ratio	–	X_1	6:1	9:1	12:1	15:1	18:1
Catalyst loading	wt.%	X_2	3	4	5	6	7
Reaction time	min	X_3	30	60	90	120	150
Reaction temperature	°C	X_4	50	55	60	65	70

Fig. 1 Representative SEM images (× 500, × 1000, and × 15,000 magnifications) of the **a**–**c** BP-600 and **d**–**f** 30K/BP-600 catalysts
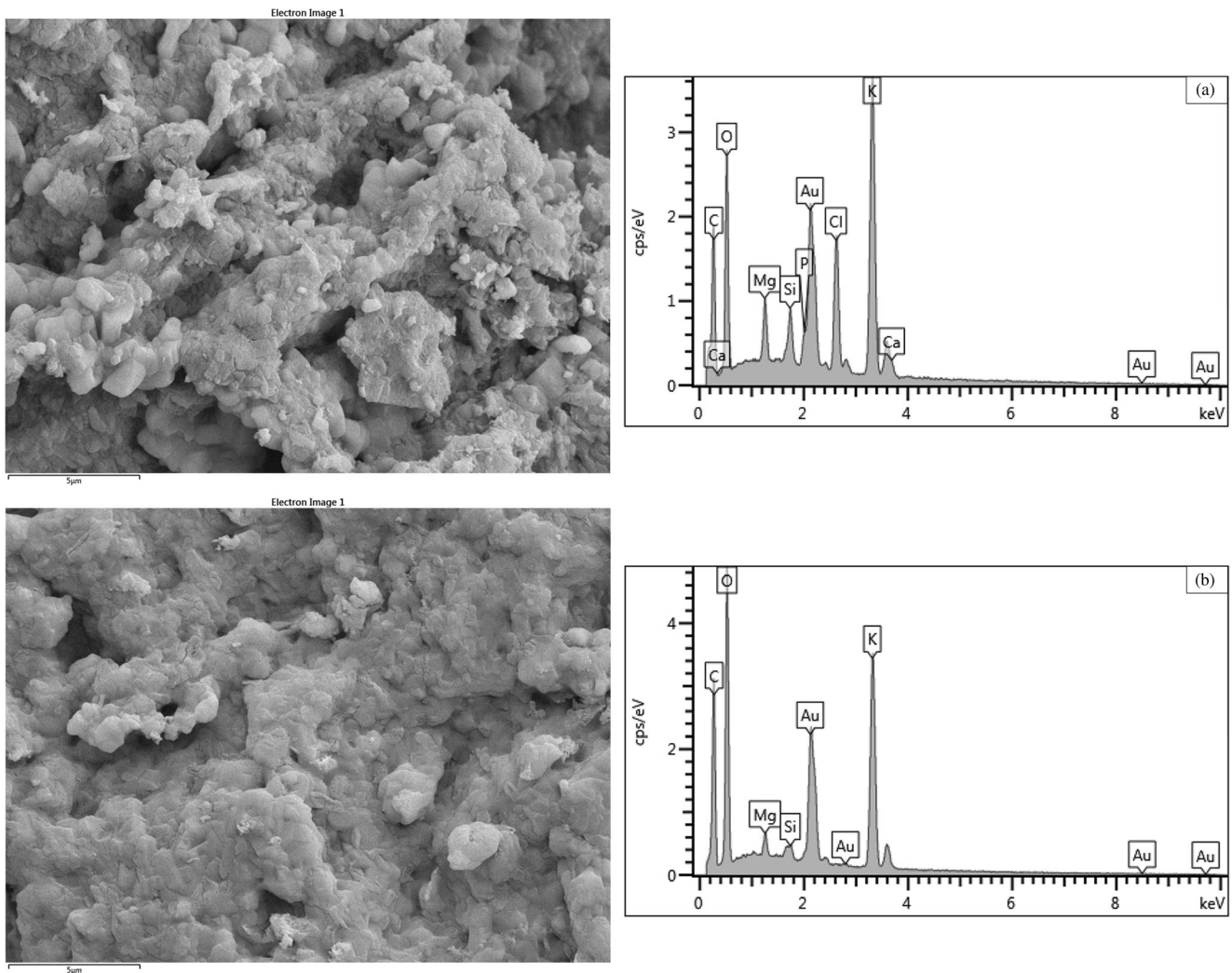

Fig. 2 Representative EDS images of the **a** BP-600 and **b** 30K/BP-600 catalysts

Table 3 Representative textural properties and EDS results of the surface of the BP-600 and 30K/BP-600 catalysts

Catalyst	Surface area (m^2/g)[a]	Total pore volume (cm^3/g)[a]	Average pore diameter (nm)[a]	Spectrum	Element content (wt.%)[b]							
					C	O	Mg	Si	P	K	Ca	Other
BP-600	36.77	0.085	12.26	1	21.30	25.19	2.13	2.08	1.55	35.43	2.03	10.28
				2	21.69	24.94	2.20	2.02	1.56	35.24	1.85	10.49
				3	21.13	25.14	2.12	2.07	1.48	35.83	1.82	10.41
30K/BP-600	26.33	0.067	9.70	1	20.59	21.38	1.21	0.73	–	56.09	–	–
				2	21.11	21.16	1.13	0.66	–	55.94	–	–
				3	20.76	21.24	1.08	0.70	–	56.22	–	–

[a] Determined by nitrogen adsorption-desorption

[b] Measured by SEM-EDX

yield of 99.5% was obtained by using RSM to set the reaction conditions as a methanol:flaxseed oil molar ratio of 5.9:1, reaction temperature of 59 °C for 33 min, and catalyst amount of 0.51 wt.% [14, 37].

This research aimed to develop a novel solid base catalyst derived from pyrolyzed cultivated banana peels as the support for a KOH catalyst for the transesterification reaction of palm oil with methanol to biodiesel (as FAMEs). The effect of the K_2CO_3 (precursor of KOH) loading level on the cultivated banana peel biochar and the effect of the calcination temperature used to prepare the catalyst were studied. Moreover, the effect of the methanol:palm oil molar ratio (6–18:1), catalyst loading level (3–7 wt.%), reaction time (30–150 min), and reaction temperature (50–70 °C) were also carefully studied. The reaction parameters were evaluated in terms of optimizing the biodiesel yield from the transesterification reaction using RSM. In addition, the physico/chemical properties of the resulting catalyst were characterized by X-ray diffraction (XRD), scanning electron microscopy coupled with energy dispersive spectroscopy (SEM-EDS), Fourier transform infrared spectroscopy (FT-IR), X-ray photoelectron spectroscopy (XPS) analyses, BET method, and the Hammett indicator method.

2 Materials and methods

2.1 Materials

Musa sapientum banana peels were obtained from local areas in Songkhla, Thailand and used to prepare the heterogeneous catalyst. Vegetable oil (palm oil) was purchased from a local supermarket in Thailand, and the physicochemical properties of the palm oil are listed in Table 1. Methanol of analytical reagent grade (99.5%) and sodium sulfate anhydrous (analytical reagent grade; 99%) were obtained from RCI Labscan Limited, while *n*-heptane (analytical reagent grade) was purchased from Fisher Scientific.

2.2 Catalyst preparation

Cultivated banana fruits were manually peeled and then the peels were cut into pieces and then washed several times with distilled water to remove the dust and impurities. They were then dried in an oven at 80 °C overnight, pulverized to powder, and sieved through 18 mesh (≤ 1 mm) to yield a fine ash. This fine ash was then calcined at 600 °C at a heating rate of 10 °C/min and held at 600 °C for 2 h under atmospheric pressure to generate the cultivated banana peel biochar. The obtained biochar was then chemically activated by suspension in 2 M KOH solution with stirring for 2 h. The suspension was filtered, washed several times with distilled water until the filtrate attained pH 7, and then dried at 105 °C for 24 h [24, 32]. The activated cultivated banana peels were named as AC.

The AC catalysts used in this experiment were synthesized using the wet impregnation method. The AC was mixed with

Table 4 Characteristics of the prepared catalysts

Catalyst	Basic strength ($H\_$)	Total basicity (mmol/g)
BP-600	$7.2 < H\_ < 15.0$	1.407
20K/BP-500	$9.8 < H\_ < 15.0$	2.551
20K/BP-600	$9.8 < H\_ < 15.0$	2.767
20K/BP-700	$9.8 < H\_ < 15.0$	2.607
30K/BP-500	$9.8 < H\_ < 15.0$	2.975
30K/BP-600	$15.0 < H\_ < 18.4$	5.012
30K/BP-700	$9.8 < H\_ < 15.0$	3.208
40K/BP-500	$15.0 < H\_ < 18.4$	4.004
40K/BP-600	$15.0 < H\_ < 18.4$	4.278
40K/BP-700	$15.0 < H\_ < 18.4$	4.481

Fig. 3 Representative FT-IR spectrum of the **a** BP-600 and **b** 30K/BP-600 catalysts
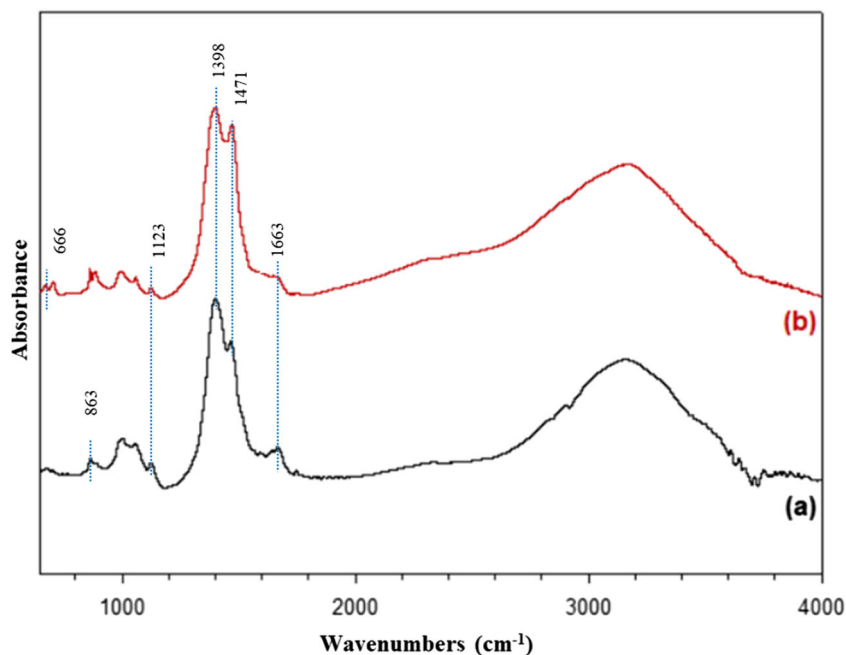

an aqueous solution containing appropriate amounts of K_2CO_3 to give a total K_2CO_3 loading of 20, 30, or 40 wt.%, respectively. In a typical process, to prepare 30 wt.% K_2CO_3 on the AC catalyst, 3 g of K_2CO_3 was dissolved in 100 mL of distillate water and subsequently 7 g of AC was added and stirred at 800 rpm for 4 h. After impregnation, the catalyst was dried in an oven at 105 °C overnight. Lastly, the catalyst was calcined in a furnace at the selected temperature (500–700 °C) under atmospheric pressure at a heating rate of 10 °C/min for 4 h to obtain the AC/KOH catalyst. The prepared catalyst was

preserved in a desiccator to avoid subsequent interaction with moisture and CO_2 in the ambient air and were named as xK/BP-T, where x and T represent the K_2CO_3 loading level (wt.%) and the activation temperature (°C) of the biochar.

2.3 Catalyst characterization

The microstructural morphology of the catalyst was recorded using SEM analysis (Oxford Aztec model) at 500, 1000, and 15,000 × magnifications with an accelerating voltage of

Fig. 4 Representative XRD patterns of the **a** BP-600, **b** 20K/BP-500, **c** 20K/BP-600, **d** 20K/BP-700, **e** 30K/BP-500, **f** 30K/BP-600, **g** 30K/BP-700, **h** 40K/BP-500, **i** 40K/BP-600, and **j** 40K/BP-700 catalysts
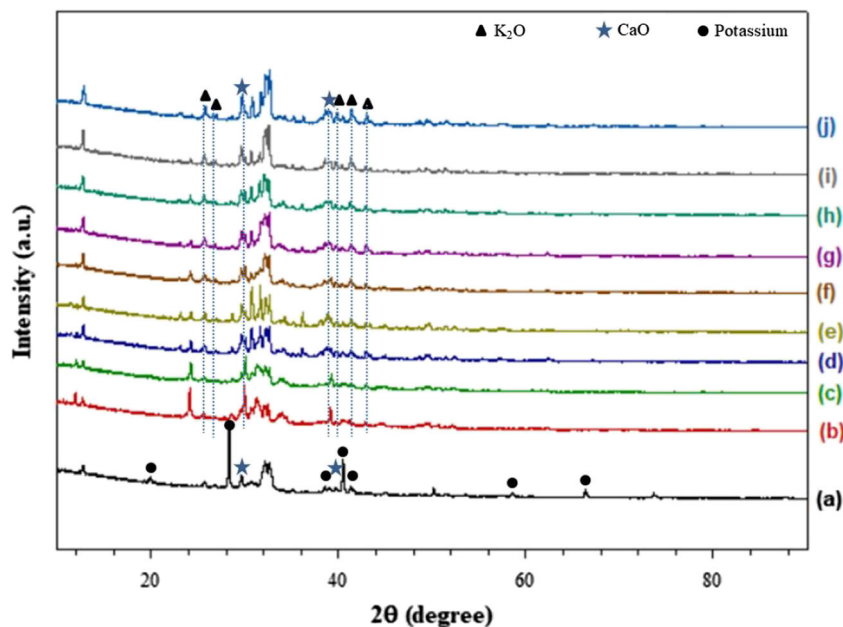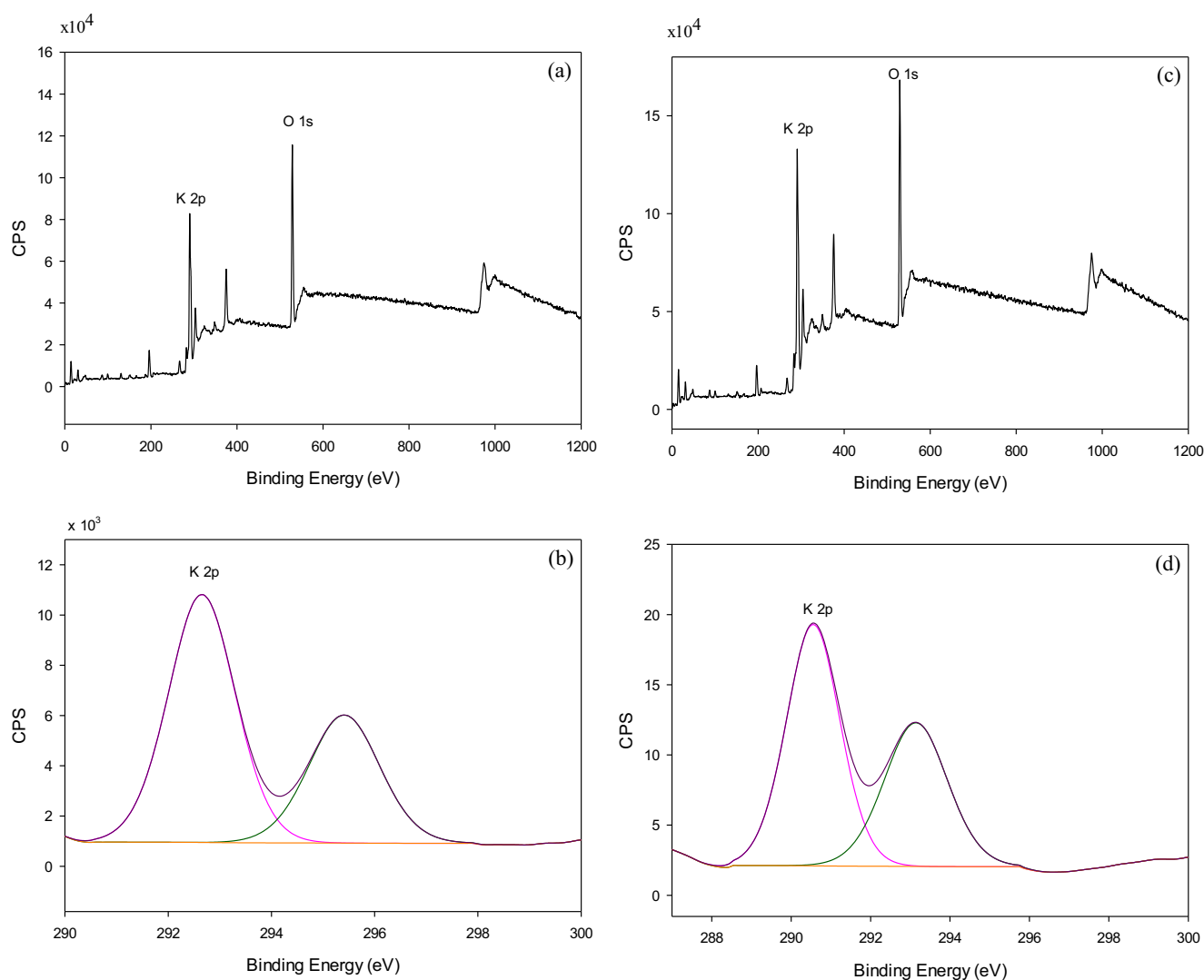
Fig. 5 Representative XPS spectra of the **a** BP-600 (wide scan mode), **b** BP-600 (narrow scan mode), **c** 30K/BP-600 (wide scan mode), and **d** 30K/BP-600 (narrow scan mode) catalysts

2.0 kV, while EDS was utilized to identify the presence of elements. The catalyst sample was placed on a stub and sputter coated with gold prior to the SEM-EDS analysis.

The specific surface area, total pore volume, and average pore diameter were calculated by nitrogen adsorption-desorption using the Brunauer-Emmet-Teller (BET) method. The volatile species that were attached on the catalyst surface were outgassed under vacuum at 250 °C overnight.

The base strength of the prepared catalyst was tested by the Hammett indicator method as the total basicity using 0.01 M benzoic acid in anhydrous methanol solution. The indicators used were as follows: bromothymol blue (H_- = 7.2), phenol-phthalein (H_- = 9.8), 2,4-dinitroaniline (H_- = 15.0), and 4-nitroaniline (H_- = 18.4).

The chemical functional group of the prepared catalyst was identified by FT-IR analysis. Powder samples were prepared by dispersing the solid sample with KBr powder and were then compressed on the form disks. The FT-IR spectrum was collected on a Perkin-Elmer spectrometer operating with a 4 cm^{-1} resolution in absorbance mode for 32 scans over a wavenumber range of 4000–650 cm^{-1}.

The internal structure, bulk phase, crystallinity and composition of the crystalline phases of the catalysts were obtained by XRD analysis. A 2.2 kW Cu anode with fine focus ceramic X-ray tube generated the Cu Kα radiation (λ = 0.15405 nm, 40 kV, 30 mA) as the X-ray source to obtain the XRD patterns, from a 2θ range of 10–90° at 5°/s.

The phase composition at the surface of the prepared catalysts was analyzed by XPS (Kratos Axis Ultra DLD) using a monochromatic Al Kα (1486.6 eV) source at 15 kV with a residual pressure of less than 5×10^{-7} Torr in the analysis chamber.
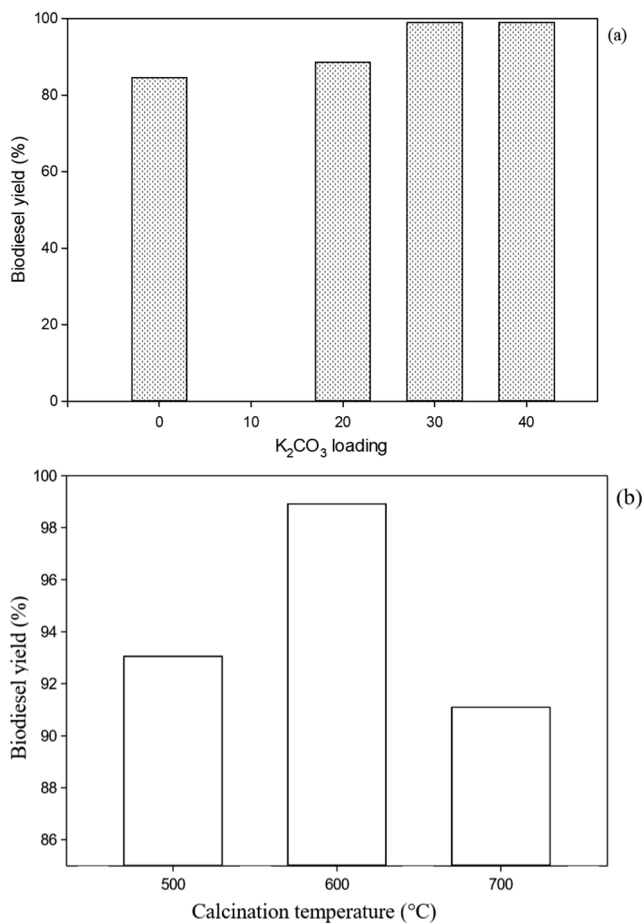
Fig. 6 Influence of catalyst preparation conditions on biodiesel yield. Reaction conditions: methanol:palm oil molar ratio, 15:1; reaction time, 120 min; reaction temperature, 65 °C; catalyst loading, 4 wt.%; **a** effect of K_2CO_3 loading level and **b** effect of calcination temperature

2.4 Experimental design

The RSM with a CCD was employed in these modeling and optimization studies to generate 27 experimental runs that were subsequently applied for designing the experiment. The total experimental runs included 16 factorials, 8 trials for axial points (two trials per variable), and 3 replicate points at the central point. The central points were repeated three times to determine the experimental error and the reproducibility of the data. The independent variables studied for the optimization of the biodiesel yield were the methanol:oil molar ratio, catalyst loading level (wt.%), reaction time (min), and reaction temperature (°C). Each variable was studied at five levels (-2, -1, 0, $+1$, and $+2$), as shown in Table 2. The experimental data obtained were analyzed by response surface regression analysis to derive a second-order polynomial quadratic equation, as shown in Eq. (1), including the main effect, quadratic effect, and interaction effect of each independent variable, to predict the biodiesel yield after the transesterification process. The response was obtained from the contour plot and

the response surface plot by designing four independent variable cases and their interactions on the biodiesel yields.

$$Y = \beta_0 + \sum_{i=1}^{k} \beta_i X_i + \sum_{i=1}^{k} \beta_{ii} X_i^2 + \sum_{i=1}^{k} \sum_{j=i+1}^{k} \beta_{ij} X_i X_j + \varepsilon \ (1)$$

where Y is the result of the response of the experiment (biodiesel yield); X_i and X_j are code factors for each independent variable (methanol:oil (molar ratio), catalyst loading level (wt.%), reaction time (min), or reaction temperature (°C)); β_0 is the general constant coefficient; β_i, β_{ii}, and β_{ij} are the linear, quadratic, and interaction constant coefficients, respectively; k is the number of variables, and ε is a random error. The analysis of variance (ANOVA) was determined via the coefficient of determination (R^2), F value, and p value and was performed in the applied Design Expert software. The regression coefficient of determination observed between the experimental and predicted biodiesel yields indicated the quality of fit for the model. Design Expert version 12 software trials (Stat-Ease Inc., Minneapolis, MN, USA) were applied for the regression analysis of the experimental data and ANOVA.

2.5 Transesterification of palm oil with methanol

Palm oil (100 g) was added into a 500-mL one-necked glass reactor on a magnetic stirring hotplate set to 65 °C or as otherwise stated. The desired amount of methanol (6, 9, 12, 15, or 18:1 M ratio of methanol:palm oil) and catalyst loading level (3, 4, 5, 6, or 7 wt.% compared with the starting palm oil) were then mixed into the palm oil until it reached the desired temperature (50, 55, 60, 65, or 70 °C) with stirring at 500 rpm for the selected time (30, 60, 90, 120, or 150 min). After that, the container was taken off the hot plate and left to cool down. The stirrer was removed and the catalyst was recovered by filtration, whereas the palm oil solution was poured into a separating funnel and left overnight for phase separation. The lower phase was removed and the upper biodiesel phase was harvested and washed with hot distilled water at 60 °C in order to remove unwanted substances. The biodiesel-water mixture was stirred at 500 rpm for 30 min, poured into a separating funnel, and allowed to phase separate. The lower unwanted phase was removed, while the upper biodiesel phase was harvested separately in a beaker. This was repeated several times until the pH of the washed water was neutral. Finally, the obtained biodiesel was kept in a glass bottle containing anhydrous sodium sulfate in order to remove the residual water.

2.6 Biodiesel analysis

The composition of the obtained FAME was analyzed by gas chromatography (GC) using a Hewlett Packard gas chromatograph 5890 Series II equipped with a flame ionization detector (FID). A DB-WAX (30 m × 0.25 mm) fused-silica capillary

Table 5 Actual and predicted values for the response surface analysis

Standard order	Standard run	Methanol:oil molar ratio (X_1)	Catalyst loading (X_2; wt.%)	Reaction time (X_3; min)	Reaction temperature (X_4; °C)	Observed FAME yield (%)[a]	Predicted FAME yield (%)	Residual
8	1	15:1 (+ 1)	6 (+1)	120 (+ 1)	55 (− 1)	99.20	98.88	0.32
7	2	9:1 (− 1)	6 (+1)	120 (+ 1)	55 (− 1)	92.80	93.53	− 0.73
2	3	15:1 (+ 1)	4 (− 1)	60 (− 1)	55 (− 1)	98.19	98.06	0.13
5	4	9:1 (− 1)	4 (− 1)	120 (+ 1)	55 (− 1)	94.21	93.50	0.71
14	5	15:1 (+ 1)	4 (− 1)	120 (+ 1)	65 (+ 1)	98.91	99.16	− 0.25
12	6	15:1 (+ 1)	6 (+1)	60 (− 1)	65 (+ 1)	94.98	95.46	− 0.48
25	7	12:1 (0)	5 (0)	90 (0)	60 (0)	93.00	93.05	− 0.05
15	8	9:1 (− 1)	6 (+1)	120 (+ 1)	65 (+ 1)	95.74	95.64	0.10
26	9	12:1 (0)	5 (0)	90 (0)	60 (0)	93.05	93.05	0.00
17	10	6:1 (− 2)	5 (0)	90 (0)	60 (0)	90.00	90.42	− 0.42
10	11	15:1 (+ 1)	4 (− 1)	60 (− 1)	65 (+ + 1)	97.83	96.69	1.14
16	12	15:1 (+ 1)	6 (+1)	120 (+ 1)	65 (+ 1)	97.93	97.91	0.02
4	13	15:1 (+ 1)	6 (+1)	60 (− 1)	55 (− 1)	99.18	99.14	0.04
20	14	12:1 (0)	7 (+ 2)	90 (0)	60 (0)	98.02	97.71	0.31
27	15	12:1 (0)	5 (0)	90 (0)	60 (0)	93.10	93.05	0.05
21	16	12:1 (0)	5 (0)	30 (− 2)	60 (0)	97.96	98.57	− 0.61
22	17	12:1 (0)	5 (0)	150 (+ 2)	60 (0)	97.92	97.95	− 0.03
19	18	12:1 (0)	3 (− 2)	90 (0)	60 (0)	97.97	98.91	− 0.94
6	19	15:1 (+ 1)	4 (− 1)	120 (+ 1)	55 (− 1)	97.97	97.83	0.14
18	20	18:1 (+ 2)	5 (0)	90 (0)	60 (0)	93.96	94.18	− 0.22
23	21	12:1 (0)	5 (0)	90 (0)	50 (− 2)	98.15	98.57	− 0.42
13	22	9:1 (− 1)	4 (− 1)	120 (+ 1)	65 (+ 1)	98.29	97.92	0.37
24	23	12:1 (0)	5 (0)	90 (0)	70 (+ 2)	99.08	99.30	− 0.22
3	24	9:1 (− 1)	6 (+1)	60 (− 1)	55 (− 1)	97.10	96.62	0.48
1	25	9:1 (− 1)	4 (− 1)	60 (− 1)	55 (− 1)	96.96	96.57	0.39
9	26	9:1 (− 1)	4 (− 1)	60 (− 1)	65 (+ 1)	98.18	98.28	− 0.10
11	27	9:1 (− 1)	6 (+1)	60 (− 1)	65 (+ 1)	96.29	96.02	0.27

[a] Determined by GC-FID

column coated with a 0.1-μm film was used. Helium gas was used as the carrier gas at a flow rate of 70 mL/min, the injector temperature was assigned at 200 °C with a split ratio of 75:1, and the detector temperature was set at 230 °C. A 0.2-μL aliquot of the FAME solution was injected at an oven temperature of 130 °C. After an isothermal period of 2 min, the GC oven was heated up to 220 °C at 2 °C/min and held for 15 min with a total run time of 62.5 min.

3 Results and discussion

3.1 Catalyst characterization

3.1.1 SEM-EDS analysis

Figure 1 shows representative SEM images of the BP-600 and 30K/BP-600 catalysts. The BP-600 catalyst displayed a lot of pores, indicating its high porosity, while the 30K/BP-600 catalyst exhibited irregular particles due to the K compounds covering the surface of the BP.

The EDS analysis of the BP-600 and 30K/BP-600 catalysts is shown as representative images in Fig. 2, and the quantitative results are summarized in Table 3. To evaluate the actual element analysis, three typical points were chosen for each sample. It was observed that the surface of the BP-600 catalyst mainly consisted of K, C, and O, while the surface of the 30K/BP-600 catalyst had a K content range from 55.94 to 56.22%, which suggested that the loaded potassium was well dispersed on the BP.

3.1.2 BET surface area analysis

The physical properties of the BP-600 and 30K/BP-600 catalysts are summarized in Table 3. The specific BET surface area, total pore volume, and average pore diameter of BP-

Table 6 ANOVA of the quadratic unreduced model for biodiesel production using calcined banana peel/K_2CO_3 as a heterogeneous catalyst

Source	Sum of squares	df	Mean square	F value	p value
Model	154.80	14	11.06	25.59	< 0.0001
X_1	21.17	1	21.17	49.00	< 0.0001
X_2	2.17	1	2.17	5.03	0.0446
X_3	0.58	1	0.58	1.35	0.2680
X_4	0.81	1	0.81	1.87	0.1969
X_1X_2	1.05	1	1.05	2.43	0.1449
X_1X_3	8.01	1	8.01	18.54	0.0010
X_1X_4	9.49	1	9.49	21.96	0.0005
X_2X_3	6.00×10^{-4}	1	6.25×10^{-4}	1.40×10^{-3}	0.9703
X_2X_4	5.31	1	5.31	12.30	0.0043
X_3X_4	7.34	1	7.34	17.00	0.0014
X_1^2	0.75	1	0.75	1.74	0.2113
X_2^2	36.94	1	36.94	85.50	< 0.0001
X_3^2	36.17	1	36.17	83.72	< 0.0001
X_4^2	46.15	1	46.15	106.83	< 0.0001
Residual	5.18	12	0.43		
Lack of fit	5.18	10	0.52	207.17	0.0048
Pure error	5.00×10^{-3}	2	2.50×10^{-3}		
Cor total	159.98	26			

$R^2 = 0.9676$; adj $R^2 = 0.9298$

X_1, methanol:oil molar ratio; X_2, catalyst loading; X_3, reaction time; and X_4, reaction temperature

Table 7 ANOVA of the quadratic reduced model for biodiesel production using calcined banana peel/K_2CO_3 as a heterogeneous catalyst

Source	Sum of squares	df	Mean square	F value	p value
Model	152.99	11	13.91	29.85	< 0.0001
X_1	21.17	1	21.17	45.43	< 0.0001
X_2	2.17	1	2.17	4.66	0.0474
X_3	0.58	1	0.58	1.25	0.2810
X_4	0.81	1	0.81	1.73	0.2080
X_1X_3	8.01	1	8.01	17.19	0.0009
X_1X_4	9.49	1	9.49	20.36	0.0004
X_2X_4	5.31	1	5.31	11.40	0.0042
X_3X_4	7.34	1	7.34	15.76	0.0012
X_2^2	45.60	1	45.60	97.88	< 0.0001
X_3^2	44.70	1	44.70	95.94	< 0.0001
X_4^2	56.44	1	56.44	121.13	< 0.0001
Residual	6.99	15	0.47		
Lack of fit	6.98	13	0.54	214.89	0.0046
Pure error	5.000×10^{-3}	2	2.500×10^{-3}		
Cor total	159.98	26			

$R^2 = 0.9563$; adj $R^2 = 0.9243$

X_1, methanol-oil molar ratio; X_2, catalyst loading; X_3, reaction time; X_4, reaction temperature

600 were 36.77 m^2/g, 0.085 cm^3/g, and 12.26 nm, respectively, and these decreased significantly to 26.33 m^2/g, 0.067 cm^3/g, and 9.70 nm, respectively, when BP-600 was loaded with 30 wt.% K_2CO_3, due to the surface and pores of the catalyst being covered with K species.

3.1.3 Basic strength

The basic strength and total basicity of the prepared catalysts were measured by the Hammett indicator method, with the results shown in Table 4. The basic strength and total basicity of the BP-600 catalyst before loading the K_2CO_3 were in the range of $7.2 < H\_ < 15.0$ and 1.407 mmol/g, respectively, suggesting the low basicity of the support. After being loaded with K_2CO_3 (from 0 to 40 wt.%), the total basicity of catalyst increased and the 30K/BP-600 catalyst exhibited the highest total basicity (5.012 mmol/g) and basic strength ($15.0 < H\_ < 18.4$). As the calcination temperature range increased from 500 to 600 °C, the total basicity of the catalyst increased, while the basic strength of the prepared catalyst remained the same.

3.1.4 FT-IR analysis

Representative FT-IR spectra of the BP-600 and 30K/BP-600 catalysts over the range of 650–4000 cm^{-1} are shown in Fig. 3. The bands observed at around 1123 and 1663 cm^{-1} were attributed to the C–O stretching and bending vibration [13]. The asymmetric stretching of the O–C–O stretching group was clearly exhibited at 1471 cm^{-1}, which was due to

the CO_2 in the air that had reacted with alkali during the preparation process [21, 24]. The peak at 666 cm^{-1} in the 30K/BP-600 catalyst was attributed to the O–H stretching and bending vibrations of water molecules adsorbed onto the surface of the catalyst. The occurrence of a peak at 864 cm^{-1} of the BP-600 catalyst represented the vibration of SiO_4 in $CaMgSiO_4$ [15]. The appearance of adsorption peaks of K_2CO_3 at 1398 cm^{-1} in the catalysts, attributed to the K_2CO_3 phase, was observed and agreed well with that of the XRD analysis [20, 32, 33].

3.1.5 XRD analysis

The XRD patterns of the BP-600 and xK/BP-T catalysts are depicted in Fig. 4. For the BP-600 catalyst, the reflection peaks at a 2θ of 19.90°, 28.33°, 38.49°, 40.48°, 41.60°, 58.59°, and 66.33°, corresponded to the characteristic peak of tetragonal structured potassium, which was found to be the main phase of the catalyst [29, 30]. Furthermore, the prominent pattern depicted intensified peaks at a 2θ of 30.68° and 39.75°, which corresponded to the CaO phase [13]. The detection of CaO was due to the ion exchange that occurred at a high calcination temperature [38]. When loaded with K_2CO_3, the intensity of the prominent peaks of these peaks gradually decreased. However, new peaks at a 2θ of 25.66°, 41.21°, 42.83°, and 44.39°, which corresponded to K_2O were detected [13, 32, 33].

Fig. 7 Predicted vs. actual biodiesel yields
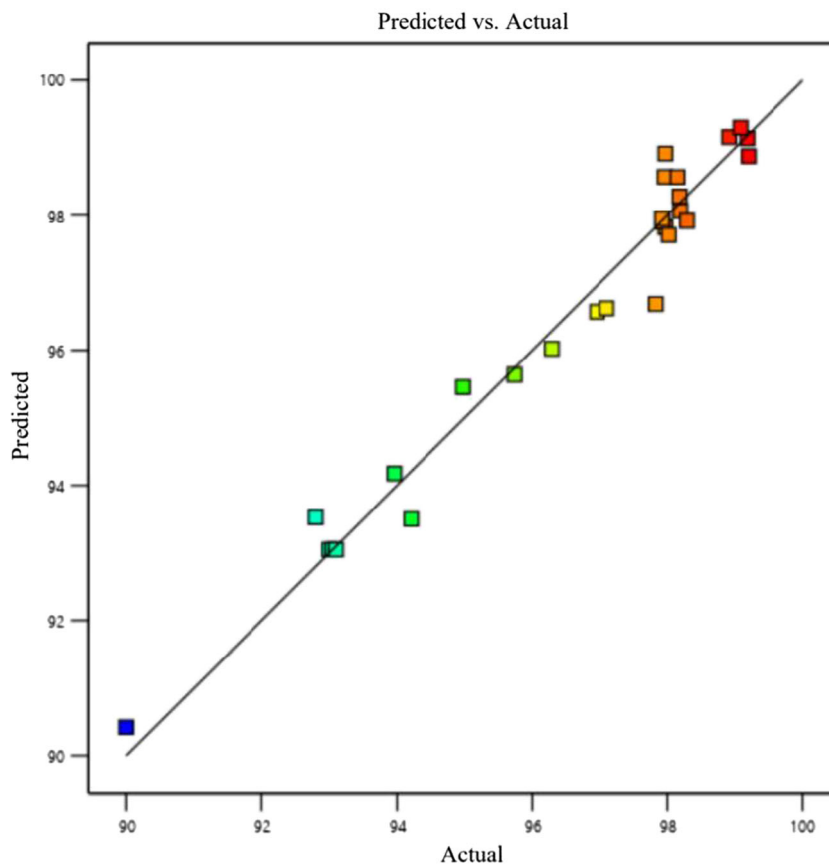
3.1.6 XPS analysis

The XPS spectra of the BP-600 and 30K/BP-600 catalysts were determined by wide and narrow scan mode, as shown in Fig. 5. The BP-600 surface exhibited an O 1s element (binding energy (BE) at 529 eV) and K 2p element (BE at 292–295 eV). For the 30K/BP-600 catalyst, it was composed of the O 1s element (BE at 529 eV) and K 2p element (BE at 291–293 eV). The result supported the SEM-EDS and XRD analyses.

3.2 Effects of the catalyst preparation conditions

Figure 6 shows the effect of the K_2CO_3 loading level. As shown in Fig. 6a, when the K_2CO_3 loading was increased from 0 to 20 and 30 wt.%, the obtained biodiesel yield increased from 84.30 to 88.50 and 98.91%, respectively, but increasing the K_2CO_3 further to 40 wt.% gave only a gradual FAME yield increase to 99%. Presumably, the K compounds agglomerated resulting in a poor dispersion of K cations on the catalyst surface [24].

Thus, the 30K/BP catalyst was selected to evaluate the relationship between the calcination temperature and the catalytic performance (Fig. 6b). As calcination temperature

increased from 500 to 600 °C, the FAME yield was markedly improved to 98.91%. Nevertheless, further increasing the calcination temperature to 700 °C decreased the biodiesel yield due to the sintering of K active sites on the catalyst surface. Therefore, the 30K/BP-600 catalyst was selected as the best catalytic activity for further study.

3.3 Statistical data analysis

The Design Expert software was used to analyze the biodiesel yields using ANOVA to estimate the influences of the methanol: palm oil molar ratio, catalyst loading, reaction time, and reaction temperature. The experimental response value was analyzed to generate the regression equation using the response surface quadratic model. The data shown in Table 5 were fitted to the CCD response surface quadratic model.

Fig. 8 Response surface plots between independent variables; **a–c** ▶ interaction effect of methanol:oil molar ratio to the **a** catalyst loading, **b** reaction time, and **c** reaction temperature; **d, e** interaction effect of the catalyst loading and **d** reaction time and **e** reaction temperature; and **f** interaction effect of the reaction time and reaction temperature
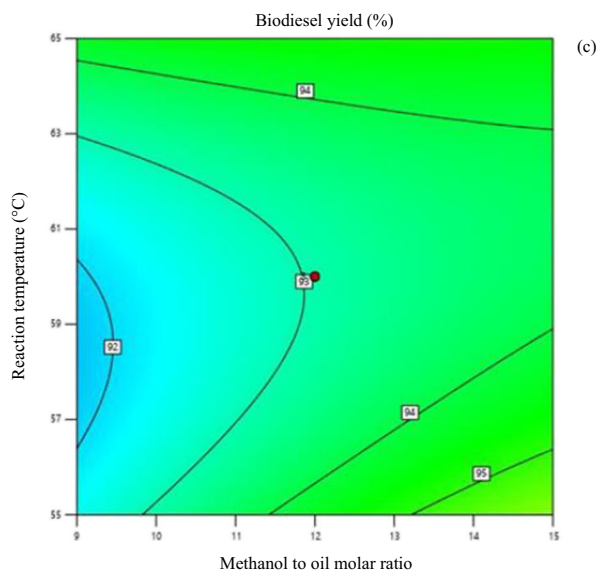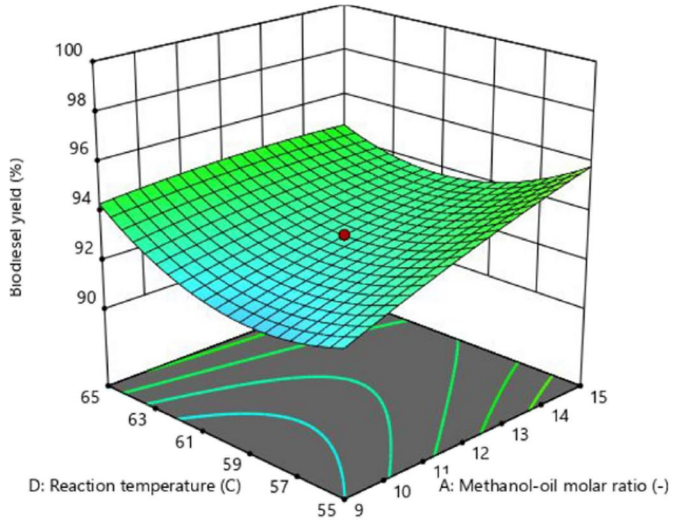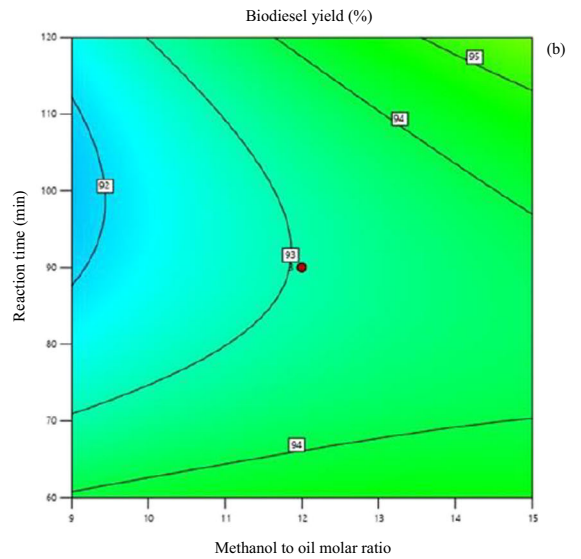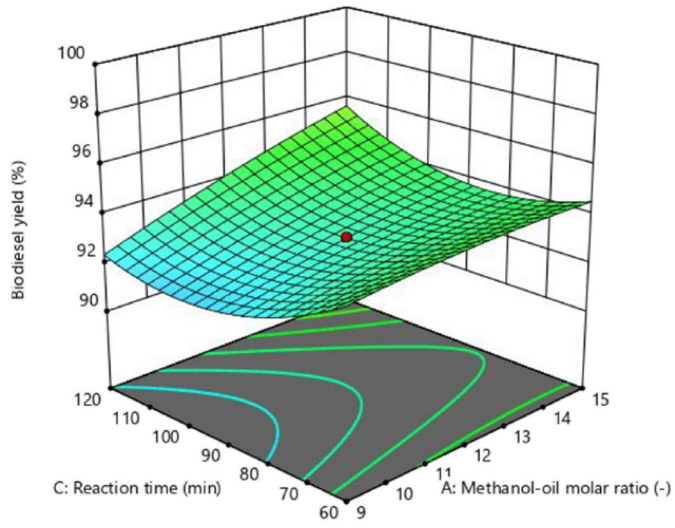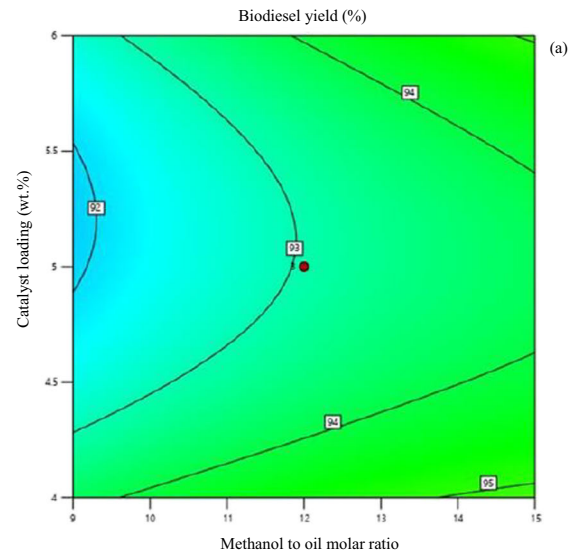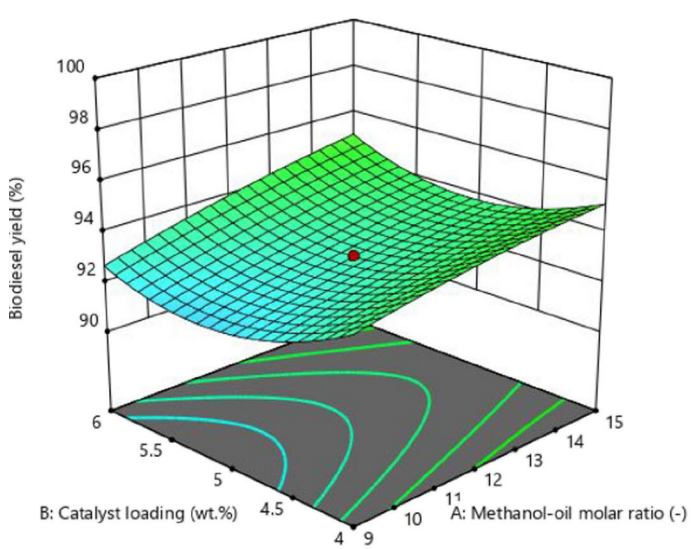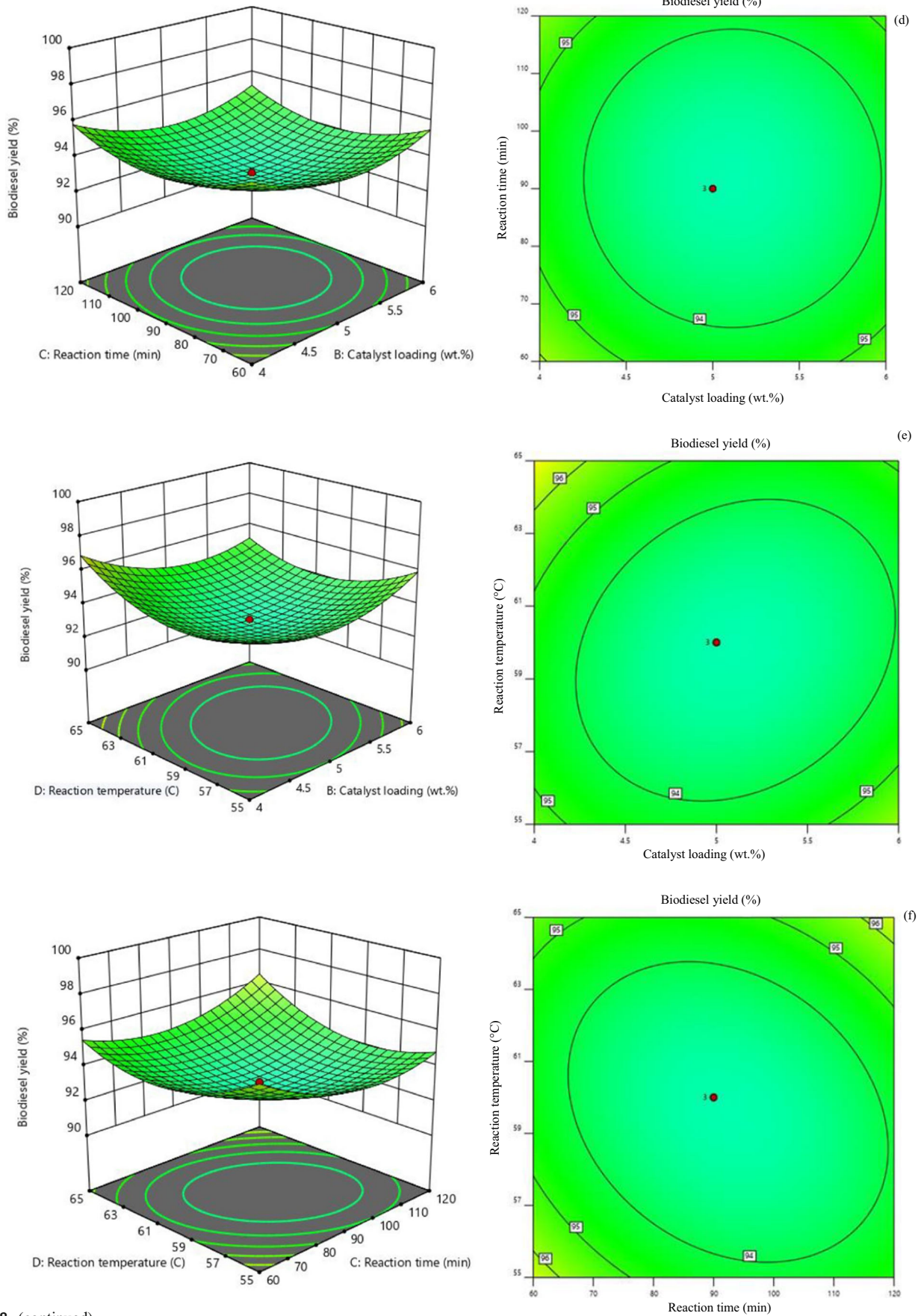
Fig. 8 (continued)

Table 8 The FAME composition of the biodiesel synthesized from palm oil using the 30K/BP-600 catalyst

FAME	Composition (%)[a]
Saturated	
C14:0	1.12
C16:0	36.61
C17:0	0.12
C18:0	3.93
C22:0	0.09
C24:0	0.10
Mono-unsaturated	
trans-C16:1	0.23
cis-C18:1	45.69
trans-C20:1	0.19
Di-unsaturated	
C18:2	10.51
Tri-unsaturated	
C18:3	0.32
Total ester content	98.91

[a] Reaction conditions: methanol:palm oil molar ratio, 15:1; reaction time, 120 min; reaction temperature, 65 °C; catalyst loading, 4 wt.%

Fig. 9 Reusability studies of the 30K/BP-600 catalyst

$$\text{Biodiesel yield} = 308.84917 + 2.75958X_1$$
$$-7.55042X_2 - 0.62990X_3 - 6.23758 X_4$$
$$+ 0.085417X_1X_2 + 0.007861X_1X_3 - 0.051333 X_1X_4 - 0.000208 X_2X_3$$
$$-0.11525 X_2X + 0.004517X_3X_4 - 0.020880X_1^2 + 1.31583X_2^2$$
$$+ 0.001447X_3^2 + 0.058833X_4^2 \tag{2}$$

where X_1 is the methanol to oil (molar ratio); X_2 is the catalyst loading level (wt.%); X_3 is the reaction time (min); and X_4 is the reaction temperature (°C).

An ANOVA test of the quadratic model in an unreduced state was used to evaluate the statistical significance term for the biodiesel yield (Table 6). The predicted biodiesel yield was exhibited in Eq. (2), where the regression was significant at the 95% confidence level (p value of the quadratic model was less than 0.05). The model F value of 25.59 and smaller p value (< 0.0001) for biodiesel production supports that the

model was significant. In this study, the X_1, X_2, X_1X_3, X_1X_4, X_2X_4, X_3X_4, X_2^2, X_3^2, and X_4^2 terms were all found to be significant.

The ANOVA fitting of the quadratic model in a reduced state for biodiesel production using calcined banana peel as a heterogeneous catalyst is demonstrated in Table 7, while the reduced quadratic model is shown in Eq. (3). The total degrees of freedom were 26. The quadratic model showed a significant regression on the model strength at the 95% confidence level. After backward elimination of insignificant terms, the result showed that the p value of the model was less than 0.05 ($p < 0.0001$), indicating that the regression terms were significant, through the main variable in the model, together with relatively high F value (29.85) and was statistically more significant. Using the model, the X_1, X_2, X_1X_3, X_1X_4, X_2X_4, X_3X_4, X_2^2, X_3^2, and X_4^2 were identified as significant regression terms (p value of the quadratic model less than 0.05). The F value of the reduced model was higher than the unreduced model for the significant regression terms. The p value for the lack of fit of the quadratic reduced model was also greater, indicating that the reduced model was more accurate when used for predicting the biodiesel production. The model showed an R^2 and adjusted R^2 of 95.63 and 92.43%, respectively.

The correlation plots between the experimental results from the transesterification experiments and the software predicted results are shown in Fig. 7. As can be seen, the graph exhibited a high correlation since the response values lie very close to the linear regression fitting.

The equation for the reduced biodiesel yield model is:

$$\text{Biodiesel yield} = 317.64023 + 2.68556X_1 - 7.17056X_2$$
$$-0.64347X_3 - 6.53825X_4 + 0.007861X_1X_3$$
$$-0.051333 X_1X_4 - 0.11525 X_2X_4 - 0.004517 X_3X_4$$
$$+ 1.37847X_2^2 + 0.001516X_3^2 + 0.061339X_4^2 \tag{3}$$

Table 9 Properties of the obtained biodiesel

Properties	Unit	ASTM D 6751	Biodiesel
Ester content	%	> 96.5	98.91
Density at 15 °C	g/cm³	0.86–0.90	0.88
Viscosity at 40 °C	mm²/s	1.9–6.0	3.62
Carbon residue	wt.%	0.050 max	0.020

3.4 Response surface plot

Figure 8a–f illustrates the experimental results from transesterification experiments by the second-order polynomial model compared with the software-predicted results of biodiesel conversion. It was observed that the actual experimental data gave a satisfactory linear regression fitting correlation with the predicted results, with R^2 and adjusted R^2 values of 96.76 and 92.97%, respectively.

In this study, the 30K/BP-600 catalyst was used for the transesterification reaction of palm oil with methanol, measuring the biodiesel (as FAMEs) yield. The response surface in the contour plots and three-dimensional plots performed by the Design Expert version 12 software trials, showed an interaction between the methanol: oil molar ratio and the (a) catalyst loading, (b) reaction time, (c) and reaction temperature, and between the reaction temperature and the (a) reaction time and (b) catalyst loading level. As mentioned, each plot was maintained at their center point levels of a 12:1 methanol:palm oil molar ratio, 5 wt.% catalyst loading, 90 min reaction time, and 60 °C reaction temperature.

3.4.1 Effect of the catalyst loading amount

As shown in Fig. 8a, d, and e, increasing the amount of catalyst significantly increased the biodiesel yield due to the increased density of basic sites (K_2O active species) in the 30K/BP-600 catalyst [13]. Similar, the biodiesel yield was reported to increase from 0 to more than 90% when the catalyst (calcined banana peel) loading was increased from 1.5 to 3.5 wt.% due to increased amount of active sites of the catalyst, but the biodiesel yield was decreased when the amount of catalyst was above 3.5 wt.% [15]. The ANOVA analysis of the quadratic reduced model (Table 7), revealed a significant interaction between the catalyst loading level and reaction temperature (X_2X_4). The optimum catalyst loading was 4 wt.% for biodiesel production.

3.4.2 Effect of the methanol:oil molar ratio

One of the essential variables influencing biodiesel yield is the methanol:palm oil molar ratio, as shown in Fig. 8a, d, and e. The high methanol: palm oil molar ratio of 15:1 used in this study resulted in a biodiesel yield of 99.2%. On the other hand, the use of a low methanol: oil molar ratio of 6:1 significantly decreased the biodiesel yield to 90.0%. This may be due to the reduced interaction between the methoxy species and the solid catalyst by increased mass transfer resistance [13, 15, 39]. From the data, the optimum methanol: palm oil molar ratio for producing biodiesel was 15:1.

3.4.3 Effect of the reaction time

The reaction time was evaluated at five levels over the range of 30–150 min using the 30K/BP-600 catalyst, as shown in Fig. 8b, d, and f, giving a biodiesel range from 90.0 to 99.2%. However, when the reaction time was increased from 120 to 180 min, the biodiesel yield was decreased due to deactivation of the active sites on the solid catalyst [30]. Thus, the optimum reaction time in this study was 120 min.

3.4.4 Effect of the reaction temperature

The reaction temperature was evaluated at five levels over the range of 50–70 °C, as shown in Fig. 8c, e, and f. A reaction temperature range between 50 and 70 °C exhibited a biodiesel yield from 90.0 to 99.2% with the optimum temperature at 65 °C.

From the ANOVA table, there was significant interaction between the methanol:oil molar ratio and the reaction time (X_1X_3) and reaction temperature (X_1X_4) between the catalyst loading and reaction temperature (X_2X_4) and between the reaction time and temperature (X_3X_4). The optimum operating parameters were predicted to be a methanol:palm oil molar ratio of 15:1, catalyst loading level of 4 wt.%, and reaction at 65 °C for 120 min, to give a biodiesel yield of 99.16%.

3.5 Physicochemical properties of the obtained biodiesel

The chemical composition of the obtained biodiesel was determined by GC-FID and is reported in Table 8. The biodiesel was composed of saturated (C14:0, C16:0, C17:0, C18:0, C22:0, and C24:0), mono-unsaturated (trans-C16:1, cis-C18:1, and trans-C20:1), di-unsaturated (C18:2), and tri-unsaturated (C18.3) FAMEs. The physic-chemical properties of obtained biodiesel were measured and compared with standard method of ASTM D 6751 and are listed in Table 9.

3.6 Reusability

Reusability of a catalyst is a very important factor for their practical application. The reusability test of the 30K/BP-600 catalyst, using the reaction conditions of: a 15:1 methanol:palm oil molar ratio, reaction time of 120 min, 65 °C reaction temperature, and 4 wt.% catalyst loading was studied. After each experimental run, the impurities attached on the catalyst surface were removed by washing with methanol and hexane, followed by drying overnight at 105 °C to eliminate residual moisture, and was then reused in the next run to evaluate the catalyst reusability. Figure 9 shows the level of conversion of palm oil to FAMEs up until the fourth cycle, where it was observed that the biodiesel yield dramatically decreased. This might be due to

Table 10 Comparison of the synthesized catalyst with other biomass-based heterogeneous base catalysts

Solid catalyst	Feedstock	Reaction condition				Biodiesel yield (%)	Reference
		Methanol:oil ratio (mol)	Catalyst loading (wt.%)	Reaction temperature (°C)	Reaction time (min)		
CaO/rice husk	Palm oil	9:1	7.0	65	240	91.5	[20]
CaO/rice husk	Palm oil	9:1	8.0	65	180	93.4	[21]
K_2CO_3/peat	Palm oil	8:1	5.0	65	90	98.6	[32]
K_2CO_3/palygorskite	Palm oil	12:1	5.0	65	210	97.0	[33]
K_2CO_3/pomelo peel	Palm oil	8:1	6.0	65	150	98.0	[34]
K_2CO_3/*Musa sapientum* ash peel	Palm oil	14.84:1	4.0	65	120	98.91	This work

the leaching of active sites on the solid catalyst during the recovery step.

3.7 Comparative study with various biomass-derived heterogeneous catalysts employed for biodiesel production

The results obtained in this study with the 30K/BP-600 catalyst in the transesterification reaction were compared in Table 10 with those previously reported. The present study exhibited a comparatively high biodiesel yield of 99.16%, with other FAME yields from 91.5–99.5% [20, 21, 24, 32, 33]. The 30K/BP-600 catalyst showed a comparable catalytic activity with other different biochar catalysts reported previously, which suggested that the 30K/BP-600 catalyst has a good potential for industrial scale use.

4 Conclusions

In summary, a novel heterogeneous AC/KOH catalyst derived from the calcination of cultivated banana peel biochar-supported K_2CO_3 for biodiesel production from palm oil was highlighted in this work. The RSM with five-level (-2, -1, 0, $+1$, and $+2$) RSM with a four-factor CCD was employed to optimize the conditions for biodiesel synthesis. The ANOVA regression models were found to be significant with a high F value (25.59) and low p value (< 0.05). The regression-reduced model was significant at the 95% confidence level ($R^2 = 0.9563$). The optimum conditions were found to be a methanol:palm oil molar ratio of 15:1, catalyst loading of 4 wt.%, reaction time of 120 min, and a reaction temperature at 65 °C to obtain a 99.15% FAME yield. In addition, the 30K/BP-600 catalyst's activity is ascribable to its high potassium content. Therefore, the 30K/BP-600 solid catalyst derived from cultivated banana peels was found to be a highly active and low-cost heterogeneous base catalyst for biodiesel production from palm oil.

References

1. Manaf ISA, Embong NH, Khazaai SNM, Rahim MH, Yusoff MM, Lee KT, Maniam GP (2019) A review for key challenges of the development of biodiesel industry. Energ Convers Manage 185:508–517. https://doi.org/10.1016/j.enconman.2019.02.019
2. Suresh M, Jawahar CP, Richard A (2018) A review on biodiesel production, combustion, performance, and emission characteristics of non-edible oils in variable compression ratio diesel engine using biodiesel and its blends. Renew Sust Energ Rev 92:38–49. https://doi.org/10.1016/j.rser.2018.04.048
3. Lam MK, Lee KT, Mohamed AR (2010) Homogeneous, heterogeneous and enzymatic catalysis for transesterification of high free fatty acid oil (waste cooking oil) to biodiesel: a review. Biotechnol Adv 28(4):500–518. https://doi.org/10.1016/j.biotechadv.2010.03.002
4. Silitonga AS, Masjuki HH, Mahlia TMI, Ong HC, Chong WT (2013) A global comparative review of biodiesel production from *Jatropha curcas* using different homogeneous acid and alkaline catalysts: study of physical and chemical properties. Renew Sust Energ Rev 24:514–533. https://doi.org/10.1016/j.rser.2013.03.044
5. Mohadesi M, Aghel B, Maleki M, Ansari A (2019) Production of biodiesel from waste cooking oil using a homogeneous catalyst: study of semi-industrial pilot of microreactor. Renew Energy 136:677–682. https://doi.org/10.1016/j.renene.2019.01.039
6. Hariprasath P, Selvamani ST, Vigneshwar M, Palanikumar K, Jayaperumal D (2019) Comparative analysis of cashew and canola oil biodiesel with homogeneous catalyst by transesterification method. Mater Today-Proc 16:1357–1362. https://doi.org/10.1016/j.matpr.2019.05.236
7. Shan R, Lu L, Shi Y, Yuan H, Shi J (2018) Catalysts from renewable resources for biodiesel production. Energ Convers Manage 178:277–289. https://doi.org/10.1016/j.enconman.2018.10.032

8. Uprety BK, Chaiwong W, Ewelike C, Rakshit SK (2016) Biodiesel production using heterogeneous catalysts including wood ash and the importance of enhancing byproduct glycerol purity. Energ Convers Manage 115:191–199. https://doi.org/10.1016/j.enconman.2016.02.032

9. Chueluecha N, Kaewchada A, Jaree A (2017) Biodiesel synthesis using heterogeneous catalyst in a packed-microchannel. Energ Convers Manage 141:145–154. https://doi.org/10.1016/j.enconman.2016.07.020

10. Tang ZE, Lim S, Pang YL, Ong HC, Lee KT (2018) Synthesis of biomass as heterogeneous catalyst for application in biodiesel production: state of the art and fundamental review. Renew Sust Energ Rev 92:235–253. https://doi.org/10.1016/j.rser.2018.04.056

11. Han S, Kim G, Han J (2019) Biodiesel production from oleaginous yeast, *Cryptococcus* sp. by using banana peel as carbon source. Energy Rep 5:1077–1081. https://doi.org/10.1016/j.egyr.2019.07.012

12. Fan M, Wu H, Shi M, Zhang P, Jiang P (2019) Well-dispersive K₂O-KCl alkaline catalyst derived from waste banana peel for biodiesel synthesis. Green Energy Environ 4(3):322–327. https://doi.org/10.1016/j.gee.2018.09.004

13. Gohain M, Devi A, Deka D (2017) *Musa balbisiana* Colla peel as highly effective renewable heterogeneous base catalyst for biodiesel production. Ind Crop Prod 109:8–18. https://doi.org/10.1016/j.indcrop.2017.08.006

14. Betiku E, Ajala SO (2014) Modeling and optimization of *Thevetia peruviana* (yellow oleander) oil biodiesel synthesis via *Musa paradisiacal* (plantain) peels as heterogeneous base catalyst: a case of artificial neural network vs. response surface methodology. Ind Crop Prod 53:314–322. https://doi.org/10.1016/j.indcrop.2013.12.046

15. Betiku E, Akintunde AM, Ojumu TV (2016) Banana peels as a biobase catalyst for fatty acid methyl esters production using Napoleon's plume (*Bauhinia monandra*) seed oil: a process parameters optimization study. Energy 103:797–806. https://doi.org/10.1016/j.energy.2016.02.138

16. Sharma M, Khan AA, Puri SK, Tuli DK (2012) Wood ash as a potential heterogeneous catalyst for biodiesel synthesis. Biomass Bioenergy 41:94–106. https://doi.org/10.1016/j.biombioe.2012.02.017

17. Ofori-Boateng C, Lee KT (2013) The potential of using cocoa pod husks as green solid base catalysts for the transesterification of soybean oil into biodiesel: effects of biodiesel on engine performance. Chem Eng J 220:395–401. https://doi.org/10.1016/j.cej.2013.01.046

18. Betiku E, Etim AO, Pereao O, Ojumu TV (2017) Two-step conversion of Neem (*Azadirachta indica*) seed oil into fatty methyl esters using a heterogeneous biomass-based catalyst: an example of cocoa pod husk. Energy Fuel 31:6182–6193. https://doi.org/10.1021/acs.energyfuels.7b00604

19. Vadery V, Narayanan BN, Ramakrishnan RM, Cherikkallinmel SK, Sugunan S, Narayanan DP, Sasidharan S (2014) Room temperature production of jatropha biodiesel over coconut husk ash. Energy 70:588–594. https://doi.org/10.1016/j.energy.2014.04.045

20. Chen GY, Shan R, Shi JF, Yan BB (2015) Transesterification of palm oil to biodiesel using rice husk ash-based catalysts. Fuel Process Technol 133:8–13. https://doi.org/10.1016/j.fuproc.2015.01.005

21. Zhao C, Yang L, Xing S, Luo W, Wang Z, Lv P (2018) Biodiesel production by a highly effective renewable catalyst from pyrolytic rice husk. J Clean Prod 199:772–780. https://doi.org/10.1016/j.jclepro.2018.07.242

22. Chen KT, Wang JX, Dai YM, Wang PH, Chen CC (2013) Rice husk ash as a catalyst precursor for biodiesel production. J Taiwan Inst Chem 44(4):622–629. https://doi.org/10.1016/j.jtice.2013.01.006

23. Zeng D, Liu S, Gong W, Wang G, Qiu J, Chen H (2014) Synthesis, characterization and acid catalysis of solid acid from peanut shell. Appl Catal A-Gen 469:284–289. https://doi.org/10.1016/j.apcata.2013.09.038

24. Zhao C, Lv P, Yang L, Xing S, Luo W, Wang Z (2018) Biodiesel synthesis over biochar-based catalyst from biomass waste pomelo peel. Energ Convers Manage 160:477–485. https://doi.org/10.1016/j.enconman.2018.01.059

25. Mendonça IM, Paes OARL, Maia PJS, Souza MP, Almeida RA, Silva CC, Jr SD, de Freitas FA (2019) New heterogeneous catalyst for biodiesel production from waste tucumã peels (*Astrocaryum aculeatum* Meyer): parameters optimization study. Renew Energy 130:103–110. https://doi.org/10.1016/j.renene.2018.06.059

26. Mendonça IM, Machado FL, Silva CC, Junior SD, Takeno ML, Maia PJS, Manzato L, de Freitas FA (2019) Application of calcined waste cupuaçu (*Theobroma grandiflorum*) seeds as a low-cost solid catalyst in soybean oil ethanolysis: statistical optimization. Energ Convers Manage 200:112095. https://doi.org/10.1016/j.enconman.2019.112095

27. Miladinović MR, Zdujić MV, Veljović DN, Krstić JB, Banković-Ilić IB, Veljković VB, Stamenković OS (2020) Valorization of walnut shell ash as a catalyst for biodiesel production. Renew Energy 147:1033–1043. https://doi.org/10.1016/j.renene.2019.09.056

28. Betiku E, Okeleye AA, Ishola NB, Osunleke AS, Ojumu TV (2019) Development of a novel mesoporous biocatalyst derived from kola nut pod husk for conversion of *kariya* seed oil to methyl esters: a case of synthesis, modeling and optimization studies. Catal Lett 149:1772–1787

29. Balajii M, Niju S (2019) A novel biobased heterogeneous catalyst derived from *Musa acuminata* peduncle for biodiesel production—process optimization using central composite design. Energ Convers Manage 189:118–131. https://doi.org/10.1016/j.enconman.2019.03.085

30. Balajii M, Niju S (2020) Banana peduncle—a green and renewable heterogeneous base catalyst for biodiesel production from *Ceiba pentandra* oil. Renew Energy 146:2255–2269. https://doi.org/10.1016/j.renene.2019.08.062

31. Wang S, Shan R, Wang Y, Lu L, Yuan H (2019) Synthesis of calcium materials in biochar matrix as a highly stable catalyst for biodiesel production. Renew Energy 130:41–49. https://doi.org/10.1016/j.renene.2018.06.047

32. Wang S, Zhao C, Shan R, Wang Y, Yuan H (2017) A novel peat biochar supported catalyst for the transesterification reaction. Energ Convers Manage 139:89–96. https://doi.org/10.1016/j.enconman.2017.02.039

33. Shan R, Shi J, Yan B, Chen G, Yao J, Liu C (2016) Transesterification of palm oil to fatty acids methyl ester using K₂CO₃/palygorskite catalyst. Energ Convers Manage 116:142–149. https://doi.org/10.1016/j.enconman.2016.02.084

34. Liu H, Su L, Liu F, Li C, Solomon UU (2011) Cinder supported K₂CO₃ as catalyst for biodiesel production. Appl Catal B-Environ 106(3–4):550–558. https://doi.org/10.1016/j.apcatb.2011.06.015

35. Osma JF, Herrera JLT, Couto SR (2007) Banana skin: a novel waste for laccase production by *Trametes pubescens* under solid-state conditions. Application to synthetic dye decolouration. Dyes Pigments 75:32–37. https://doi.org/10.1016/j.dyepig.2006.05.021

36. Tan YH, Abdullah MO, Hipolito CN, Zauzi NSA (2017) Application of RSM and Taguchi methods for optimizing the transesterification of waste cooking oil catalyzed by solid ostrich and chicken-eggshell derived CaO. Renew Energy 114:437–447. https://doi.org/10.1016/j.renene.2017.07.024

37. Ahmad T, Danish M, Kale P, Geremew B, Adeloju SB, Nizami M, Ayou M (2019) Optimization of process variables for biodiesel production by transesterification of flaxseed oil and produced biodiesel characterizations. Renew Energy 139:1272–1280. https://doi.org/10.1016/j.renene.2019.03.036

38. Chen G, Shan R, Shi J, Liu C, Yan B (2015) Biodiesel production from palm oil using active and stable K doped hydroxyapatite catalysts. Energ Convers Manage 98:463–469. https://doi.org/10.1016/j.enconman.2015.04.012

39. Jitjamnong J, Luengnaruemitchai A, Samanwonga N, Chuaykarn N (2019) Biodiesel production from canola oil and methanol using Ba impregnated calcium oxide with microwave irradiation-assistance. Chiang Mai J Sci 46(5):987–1000